Jurnal Kejuruteraan 31(2) 2019: 229-241
https://doi.org/10.17576/jkukm-2019-31(2)-07

Effects of Nanopowder Addition on Rheological Properties of Feedstock for Micropowder Injection Moulding Process

Javad Rajabi[a*] & Abdolali Fayyaz [b]
[a]*Department of Mechanical Engineering, Gonbad Kavoos Branch, Islamic Azad University, Gonbad Kavoos, Iran*
[b]*Department of Materials Engineering, Science and Research Branch, Islamic Azad University, Tehran, Iran*
**Corresponding author: rajabi.javad@gmail.com*

Received 29 October 2018, Received in revised form 16 January 2019
Accepted 15 May 2019, Available online 31 October 2019

ABSTRACT

Micropowder injection moulding (μPIM) is an ideal alternative for miniaturization of parts because of its ability to produce complex micro-geometries at low manufacturing cost. Utilizing bimodal powder mixtures in feedstock can increase packing density and densification of parts fabricated via μPIM. This study investigated the feedstock consists of nano-micro 316L stainless steel powder-and polyethylene glycol-based binder system. The flowability of different feedstocks was evaluated using rheological parameters, including critical powder volume concentration (CPVC), melt viscosity, activation energy, and rheological index. Results showed that mixing nanopowders with micropowders increases CPVC from 67.66 vol.% (pure micropowder) to 78.33 vol.%. The nano-micropowder feedstock showed viscosity below 45 Pa·s and shear rate in the range of 102 s^{-1} to 105 s^{-1}, which are suitable for the μPIM process. The determined flow index values ranged from 0.25 to 0.76, and the reduced n values at high temperature with the addition of nanopowder indicated a possible increase in shear-thinning behavior. A defect-free microsample was obtained at an injection temperature of 85°C with sintering at 1200°C. Using the nano–micro bimodal powders, the hardness of the obtained samples also increased from 182 HV to 221 HV, with strength of 501 MPa, which is higher than that of the sample obtained with the use of micropowder only (435 MPa).

Keywords: Micropowder injection moulding; Rheology; Flow behavior; Flow index; Nanopowder

INTRODUCTION

Micropowder injection moulding (μPIM) has been developed in powder metallurgy among promising cost-effective methods for the mass production of small-scale intricate sections. μPIM has five main subprocesses, namely, selection of raw materials (powder/binder), feedstock preparation, injection moulding, debinding, and sintering (Javad et al. 2012; Quinard et al. 2009). The success of μPIM highly depends on feedstock (powder–binder mixture) characteristics. Feedstock shows pseudoplastic behavior, in which viscosity declines when the shear rate increases at a certain temperature. The feedstock with the lowest activation energy (E), the highest mouldability index and the highest value in terms of shear sensitivity (n-1) is the most appropriate feedstock for injection moulding (Abolhasani & Muhamad 2010; German & Bose 1997; Merz et al. 2002). Similar to pure polymers, μPIM feedstock often exhibits pseudoplastic (shear thinning) flow behavior, in which melt viscosity reduces when the shear rate decreases; viscosity likewise decreases when temperature increases (Attia & Alcock 2011; Emeka, et al. 2017; Ismail et al. 2008). Feedstock homogeneity occurs at a low mixing torque, considering that the binder material and powder are easily mobilized. Based on torque and rheological analyses, a higher torque is also indicative of a higher viscosity.

Prior studies showed that fine powders are advantageous in a suspension given their enhanced densification behavior and high surface area (Trunec & Maca 2007; Trunec et al. 2008). For example, Trunec and Maca (2007) showed an increase in sintered density by reducing the particle size of zirconia. However, smaller particles also agglomerate, increase mixture viscosity, and reduce powder loading (Huang et al. 2005; Wetzel et al. 2005). In the preceding studies, the advantages of employing a broad variety of particle size distribution where vacant spaces in between large particles can be occupied with small particles, have been also examined (Hashim et al. 2002; Suri et al. 2003). Different bimodal mixture models have been proposed to predict particle packing behavior (Martin & Bouvard 2004; Shi & Zhang 2000). However, their applicability to nanopowders, in which agglomeration dominates, has not received much attention, specifically from the perspective of powder processing into net-shaped architectures. The main aim of this study is to examine the effects of adding a fraction of nano-scale stainless steel 316L powder on the mixing and rheological behavior of the bimodal nano–microsized powder feedstock.

METHODOLOGY

In this work, water-atomized 316L stainless steel powders with an average particle size of 150 nm and 5 μm (as reported by the supplier) were used. The particle size distribution of

the micropowders was confirmed by Malvern Mastersizer 2000, whereas that of the nanopowders was verified using Malvern Zeta Sizer. The binder system was composed of 75% polyethylene glycol (PEG), 25% polymethyl methacrylate (PMMA) and 2% stearic acid (SA). To analyse the thermal properties of the binder, the degradation temperature and melting point of the binder components were measured via thermogravimetric analysis (TGA) and differential scanning calorimetry (DSC), respectively.

A planetary ball mill (Fritsch Pul-verisette-6) was used to obtain a homogeneous nano- and micropowder mixture. To evaporate ethanol, the mixed powders were dried in a vacuum oven at 100°C for 24 h. The critical powder volume concentration (CPVC) was determined using oil absorption technique (ASTM D-281-31), in which 0.5 ml of oleic acid was added every 5 min until the mixture reached its maximum torque (Javad et al. 2013). The feedstock was prepared using Brabender mixer (GmbH & Co., KG) with a rotation frequency of 30 rpm. In this study, PMMA was utilized in form of emulsion (PMMA and acetone) because previous studies [20, 21] showed that a PMMA emulsion contributes to the fabrication of more homogeneous feedstocks with lower viscosity in comparison with PMMA powder (Jamaludin et al. 2009; Ibrahim et al. 2010). Rheological properties was measured using a capillary rheometer (Shimadzu CFT-500D) according to use in the study of feedstock rheology with capillary size L/D = 10 as the standard for measuring the shear rate and viscosity of the feedstocks (ASTM Standard D 3835-02). µPIM was performed using a µPIM machine (DSM Xplore). Solvent debinding process was performed using a MEMMERT water batch. The test was performed at 50°C. The samples were immersed in water for 1 h to 6 h. Debinding and sintering of the debinded parts were performed in a high-vacuum sintering furnace (Korea VAC-TEC type Model VTC 500HTSF). Hardness testing was also performed to verify the hardness of the sintered parts using a MITAKA machine on the polished surface.

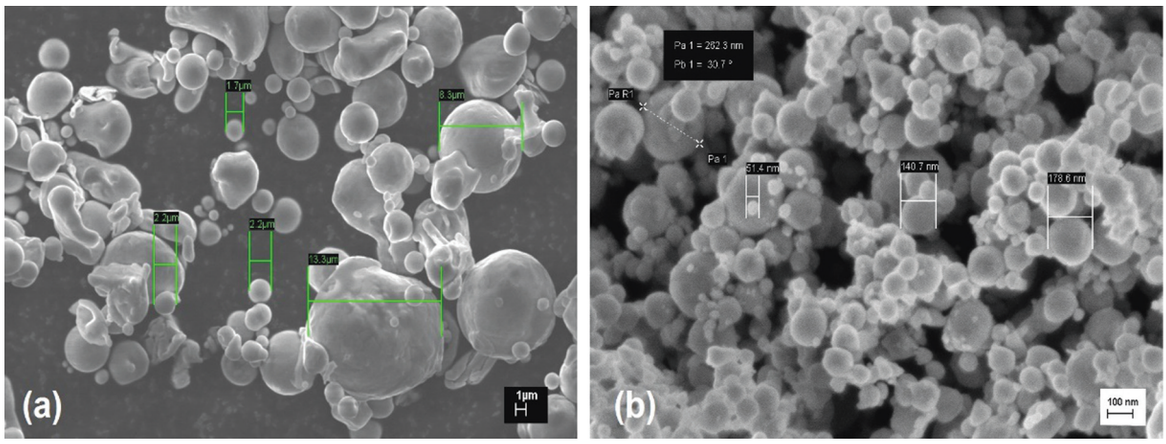

FIGURE 1. SEM images of SS316L (a) micro, (b) nano-sized powder

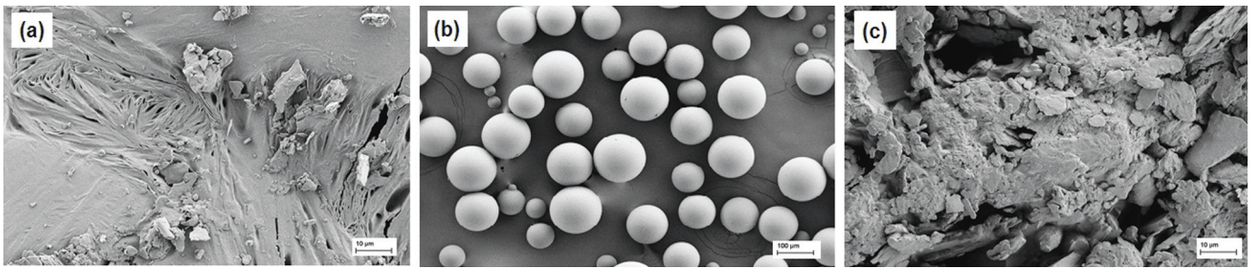

FIGURE 2. SEM images of (a) PEG (b) PMMA (c) SA

RESULTS AND DISCUSSION

CHARACTERISATION OF MATERIALS

Figure 1 shows the SEM images and particle size distribution of micro- and nanosized SS 316L powders. The average diameters of the micro- and nanosized SS316L powders were approximately 5 µm and 401 nm with irregular and spherical shapes, respectively. Supplier technical specification report and analysis in the size of the nanopowders differed because nanosized powders agglomerate because of their high surface area. Therefore, the nanopowders should be de-agglomerated by milling and heating prior to mixing with the binder. The chemical composition of the metal powder is also given in Table 1.

TABLE 1. Powders composition

Element	Wt.%	
	Micro	Nano
C	0.028	0.031
Si	0.59	0.61
Cr	15.13	16.89
Mn	3.41	1.55
Ni	10.08	11.09
Mo	1.74	2.03
Fe	Balanced	

TABLE 2. Composition of binder system

Binder	Melting point (°C)	Degradation temp (°C)	Density (g/cm^3)
PEG	63	431.2	1.23
PMMA	127.73	406.1	1.19
SA	60.64	308	0.94

Figures 2(a) to 2(c) shows the SEM images of PEG, PMMA, and SA binders, respectively. The melting points and degradation temperatures of PEG, PMMA, and SA are given in Table 2. The melting point of PEG, PMMA, and SA were 63, 128, and 61°C, respectively. The TGA curve shows that these substances decompose between 308°C to 430°C. Given that one component shows the highest melting point, for the binder system of PEG/PMMA/SA, mixing can occur at above 128°C, and the critical temperature for debinding is at 430°C.

PRE-MIXING OF NANO AND MICROPOWDERS

Figure 3 shows the SEM image of mixed powders after ball milling with different addition nano-sized powder to micro-sized powder. The main aim of ball milling to the mixing of nano and micro powders was to deagglomerate nano powders and to achieve an appropriate distribution of the mixture. German and Park (2008), who studied bimodal powder mixtures, reported that improving the packing density of a powder can be achieved by adding considerably smaller particles that fill the voids among

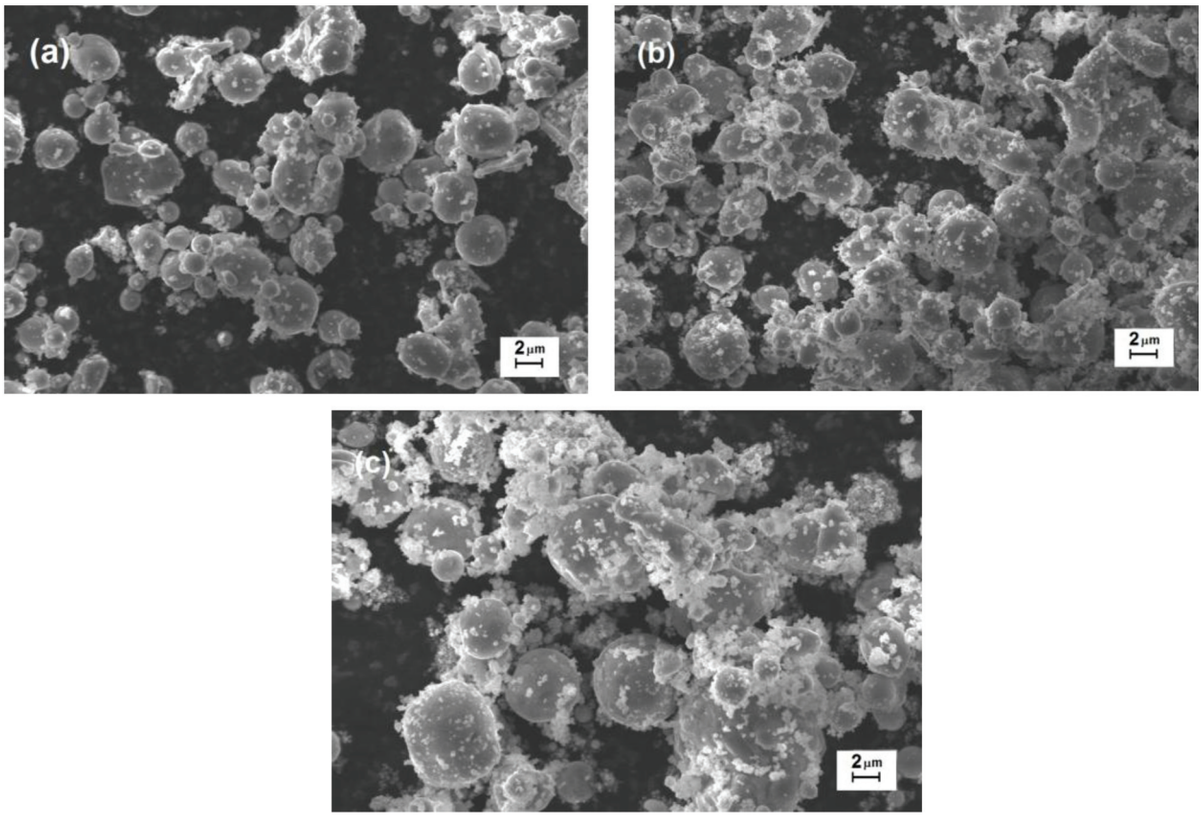

FIGURE 3. SEM image of mixed powders (a) 10 wt. % nano (b) 20 wt. % nano (c) 30 wt. % nano

the larger particles. Small quantities of smaller powders improve density, but an excessive amount of the smaller powder may be counterproductive. Apart from reducing the price of the powder mixture in comparison to that of pure nanopowder, mixing irregular-(micro) and spherical (nano)-shaped powders also increases the strength in debound parts according to German and Bose (1997). In their work, wet milling method was used to de-agglomerate and produce a homogenous nano-micro powder mixture. The main reason is that nanopowders must be well distributed between micropowders. In addition, an irregular micropowder, which constituted the main portion of the mixture, was selected

because it offers low price and endows high strength in the brown parts.

The density of bimodal powders is given in Table 3. As shown in Table 3, bimodal powders with larger nanopowders have lower apparent and tap densities (3.85 gr/cm^3 and 2.24 gr/cm^3, respectively) but have higher pycnometer density (7.73 gr/cm^3) because of their high surface area. This value is due to the high volume of the powder. This result shows that packing density can be improved using nanopowder addition in nano-micro hybrid powder mixture compared with monomodal powder systems, which include pure nano- or micropowder. This finding is relevant in fabricating components using powder metallurgy and PIM. Sintering and densification provide better results at lower temperature because of these processes produce more contact surfaces and decreased porosity.

TABLE 3. Density of bimodal powder mixtures

Sample (wt.% nano)	Density(gr/cm^3)		
	Apparent	Tap	Pycnometer
10	2.67 ± 0.2	4.55 ± 0.17	7.35 ± 0.26
20	2.47 ± 0.24	4.17 ± 0.21	7.48 ± 0.23
30	2.24 ± 0.18	3.85 ± 0.19	7.73 ± 0.24

Given that density is equal to mass divided by volume, when two powders are mixed, the sum of the mass is divided by the sum of the volume to calculate the mixture theoretical density, as shown in Equation 1.

$$\left(\frac{1}{\rho_T}\right)=\left(\frac{W_L}{\rho_L}\right)+\left(\frac{W_S}{\rho_S}\right) \quad (1)$$

where ρ_T is the theoretical density of the mixture, which consists of W_L, the weight fraction of large-sized powder with density ρ_s, and W_S, the weight fraction of small-sized powder with a theoretical density of ρ_s. Determining the weight fractions is the most typical method to calculate the theoretical density of a mixture. The method considers the case of a hybrid nano-micro mixed powder with different sizes and densities. The pycnometer density of powder mixtures is calculated using the inverse rule of mixtures based on Equation 1, as shown in Figure 4. According to experimentally achieved pycnometer density and calculated density using Equation 1, the homogeneity of the mixture was found to exceed 90% $\left(\frac{\rho_{exp}}{\rho_{theo}}\times 100\%\right)$, which revealed good distribution and homogeneity among nano- and micropowders. Notably, a mixture with good homogeneity can facilitate in obtaining uniform properties of the final parts.

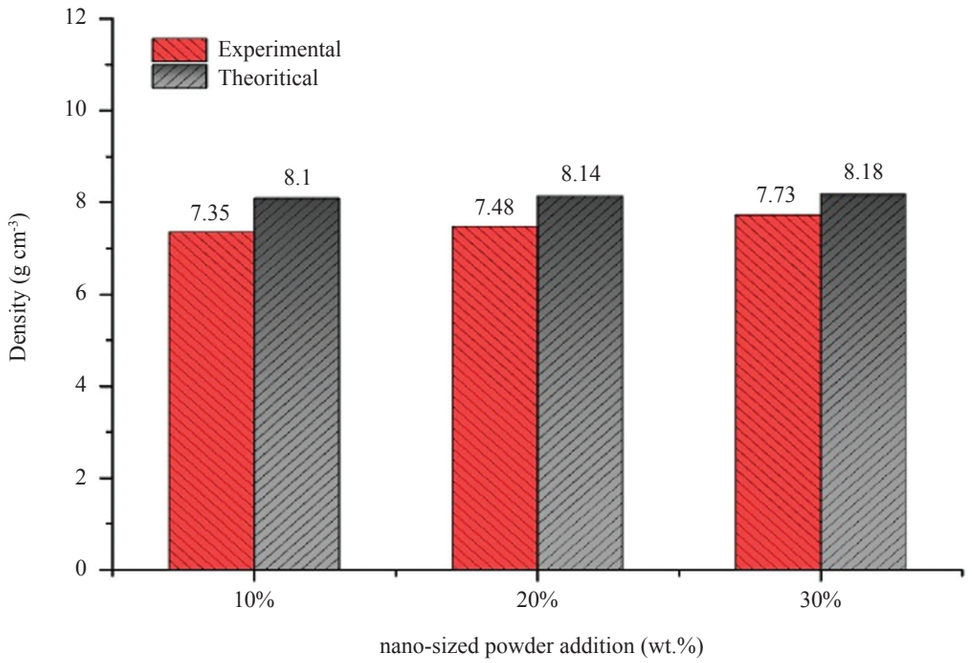

FIGURE 4. Comparison between experimental and theoretical pycnometer density

THE CRITICAL POWDER VOLUME CONCENTRATION (CPVC)

Figure 5 represents the mixing torque as a function of time for incremental powder additions for micro SS 316L powders to determine CPVC. CPVC is the point where the particles are tightly packed, and all voids between the particles are filled with binder. The correlation between powder volume and oleic acids is calculated using Equation 2:

$$CPVC = 100\times\frac{V_f}{V_f + V_o}\% \quad (2)$$

where V_f is volume of powder (cm^3) and V_o is volume of oleic acid (Harun et al. 2010).

Figure 5 demonstrates the change of mixing torque value in Nm for incremental powder addition of µ-SS 316L powders as time passes by. As can be seen in the picture, after any addition, there comes a sudden jump in mixing torque's trend followed by hovering at a lower value as soon as the homogeneity level of the mixture reaches to its maximum possible point at the shear rate. Moreover, as the powder content increases, the mixing torque also increases up to a critical point (67.6 vol.%). Additionally, an excess of powder in the mixture appeared as a cut down of the mixing torque.

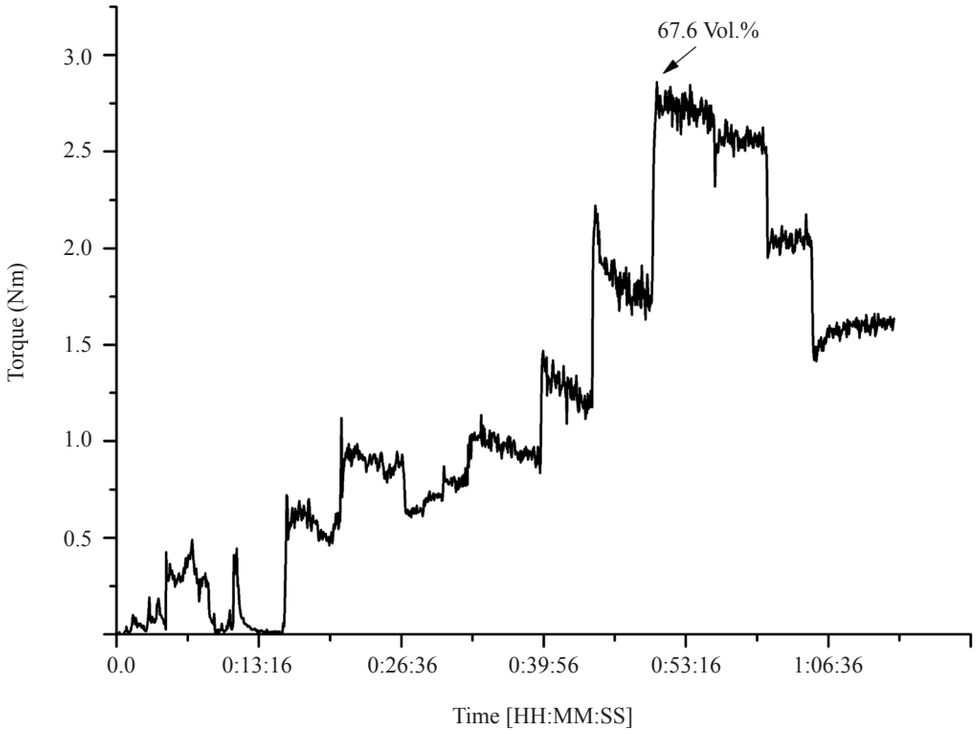

FIGURE 5. The mixing torque as a function of time of µ-SS 316Lpowder-oil mixture

Notably, low CPVC and less binder amount resulted in increased viscosity and the formation of trapped air pockets that presented moulding difficulties. During debinding, these voids cause cracking, and thus a deficiency of binder is unacceptable. By contrast, excess binder can cause separation of the binder from the powder during moulding, which leads to flashing in the moulded component and green part slumping during debinding. Figure 6 presents the effect of the addition of nanopowder on the CPVC values. Mixing nanopowder with micropowder resulted in increased CPVC compared with that of micropowder from 67.66 vol.% to 78.33 vol.%. This means that broad particle size distributions or bimodal distributions are desirable to maximize the solid loading, since the small particles fill interstitial spaces and the release binder (oil) to lubricate the particle flow (German & Bose 1997).

When particle size increases as a result of low surface area, less binder is needed to cover the surface of powders. However, once nanopowder is added to the micropowders, the binders between spaces of micropowders are removed and superseded by nanopowders (Figure 7). In bimodal systems involving nano- and micropowders, powder loading is increased in comparison with pure micropowders.

MIXING OF POWDER AND BINDER

The optimal powder loading for injection should be less than the CPVC. At this point, the feedstock (powder–binder mixture) has sufficiently low viscosity for moulding but exhibits good particle-particle contact to ensure shape preservation during processing. The slight excess of binder over that at the CPVC provides needed lubricity for moulding. At the CPVC, the feedstock has very high viscosity. A slight excess of binder of around 2% to 5% is necessary to provide lubricity for moulding (German & Bose 1997). Therefore, in the present work, powder loading of around 62% was considered for mixing powders with a binder system. In the next step, powder loading increased to 65% for samples that consist of 20% and 30% nanopowders according to their CPVC. Given the high viscosity in high powder loading, a low viscosity feedstock is required to fill the fine cavity in the µPIM process. Therefore, powder loading above 65% was not considered. Reports about µPIM showed that powder loading used for SS 316L feedstock is usually less than 65% (Ibrahim et al. 2009; Ibrahim et al. 2010; Quinard et al. 2009).

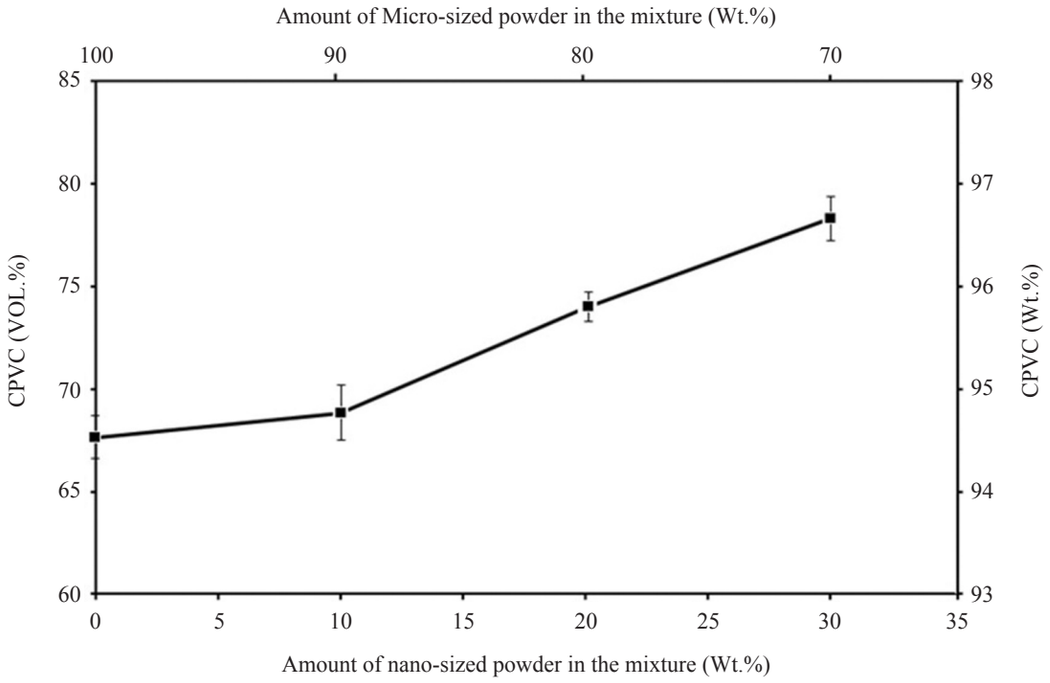

FIGURE 6. The effect of nano-sized powder addition on the CPVC value

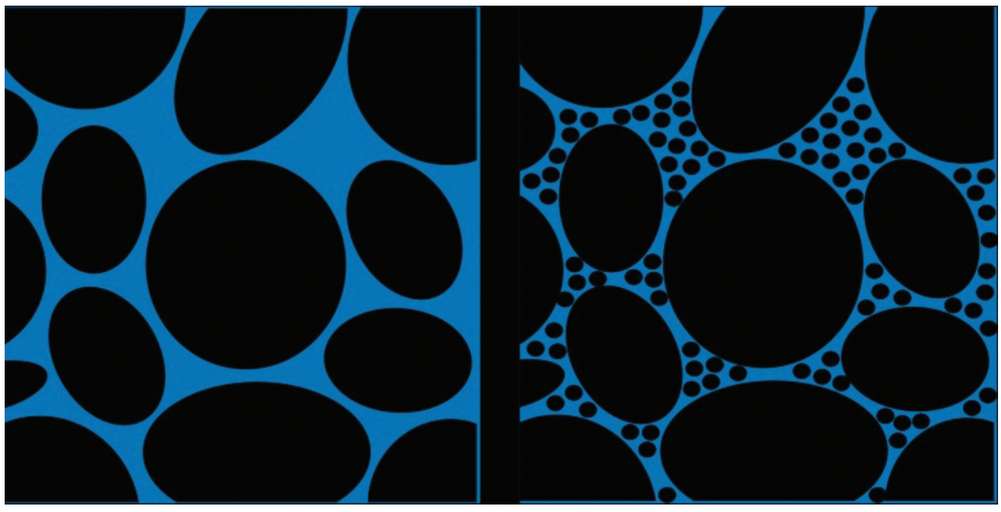

FIGURE 7. The schematic of filling of space among micro powders by nano powders

EFFECT OF THE ADDITION OF NANOPOWDER

SEM images were obtained from the monomodal and bimodal samples in order to observe any increase in powder content as the nanopowder is added to it (Figure 8). By looking at figure 8, it can easily be noticed that the binder uniformly scattered across the feedstock, and a thin layer of the binder is formed around almost all the metal particles, even for nanopowders in bimodal powder mixtures. In addition, the nanopowder fits into the interstitial spaces between the micropowder, and the particle–binder mixture depicts a fully compact structure with no pores (Figures 8(b) to 8(d)). Mixing torque is plotted as a function of solids loading in Figures 9(a) to 9(d) for the monomodal and bimodal systems. We found that mixing torque generally decreases by adding nanosized particles in mixtures. This behavior can be attributed to the decreased suspension viscosity in bimodal mixtures, which is possibly due to the higher packing capability observed in bimodal mixtures, leading to lesser hydrodynamic friction between the powder and polymer phases (Onbattuvelli et al. 2013). In addition, given the shape irregularity in the microparticles, mixing torque values can be increased at a comparable solids loading.

As shown in Figure 9, when the powder is introduced, the torque increases to a high level, because the powder is cold and poorly distributed in the binder. With continued

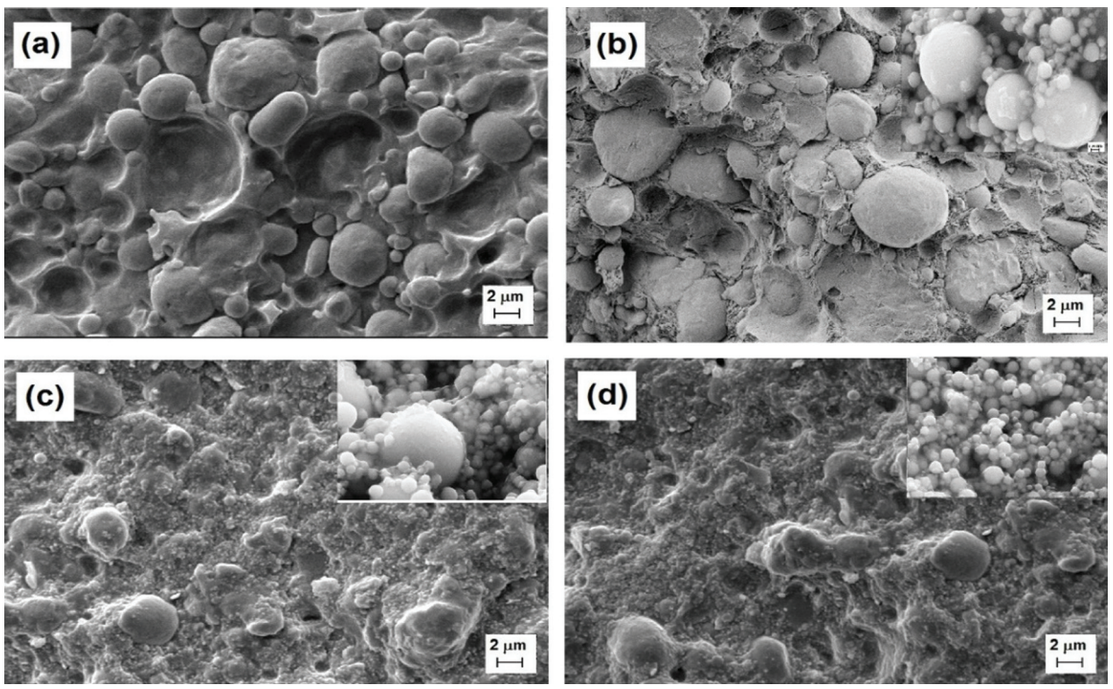

FIGURE 8. SEM image of feedstock (a) micro powder (b) nano powder (10%) (c) nano powder (20%) d) nano powder (30%) in PEG binder system

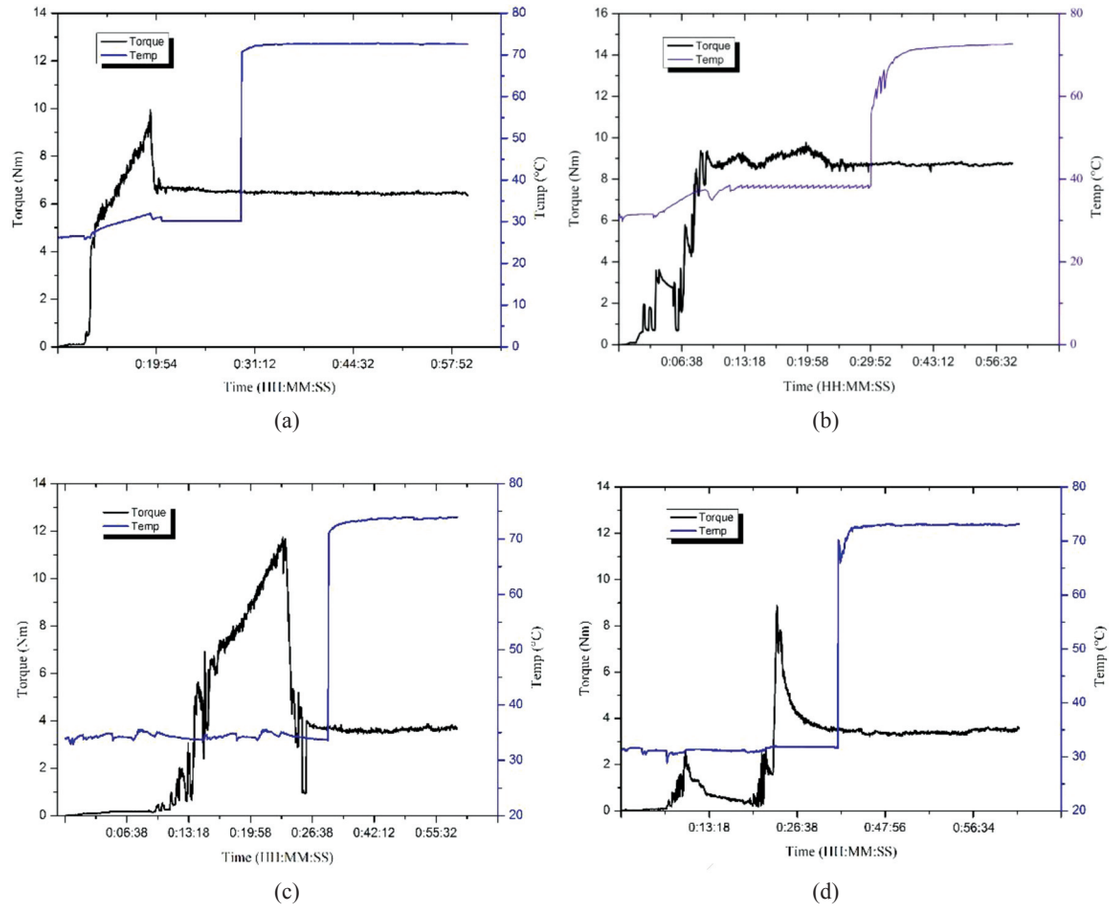

FIGURE 9. The effect of nano-sized powder addition on the Torque (a) micro powder (b) 10% nano powder (c) 20% nano powder (d) 30% nano powder in PEG feedstock

shear, the torque reaches a steady-state value that indicates homogeneity. Notably, an erratic torque is an indication of poor mixture homogeneity of a solid loading that is greater than the CPVC. During mixing of the powder with the binder, the temperature typically increases by 15°C to 20°C beyond the set point because mechanical mixing work and the homogeneity of the mixture can be sensed by monitoring the torque (German & Bose 1997). Mixing torque can also be used to achieve homogeneity during mixing, in which the resistance to continued shear versus mixing time is assessed. As seen in Figure 9, the torque decreases as agglomerations are broken and as the binder becomes better dispersed in the mixture.

The best approach is to mix the surfactant with the powder right before mixing it with the binder as has been utilized in this work. Because during the mixing procedure, the surface-treated powder is added to molten binder and capillary action makes the liquid to be wicked into particle clusters. This action resulted in the lubrication of the particles and a continual de-agglomeration of clusters. Notably, contamination increases with mixing time, which is a key reason for the short mixing times. Mixing at an excessively high temperature also degrades the binder or allows powder separation because a low mixture viscosity results in a density gradient within the feedstock.

EFFECT OF THE POWDER LOADING

Figure 10 presents the changes in torque as a function of mixing time for different powder loadings. Powder concentration significantly affects the torque evaluation curves. Two powder loadings ranging from 62 vol.% to 65 vol.% were evaluated by using PEG binder systems. The mixing torque which is proportional to the shear stress of mixer shows that the emitted work energy is used to distribute and also scatter the powder in the binder. By the way, the time taken for the mix to achieve this steady state is called mixing time. It can be seen that the torque increases with the increase of the powder loading from 62 vol.% to 65 vol.%. This phenomenon clarifies that the higher the amount of powder loading, the greater the friction will be and it leads to higher viscosity of the mixture. For 65 vol.% powder loading, the torque stabilizes at a steady level in a short time, indicating uniform mixing. By contrast, 62 vol.% powder loading took longer time to obtain a stabilized torque value because of more binder, which indicates that homogeneous mixing is attained with a longer mixing time of 30 min. Feedstock with the highest powder loading possible is generally advantageous to obtain high green density and strength, as well as to minimize subsequent sintering shrinkage.

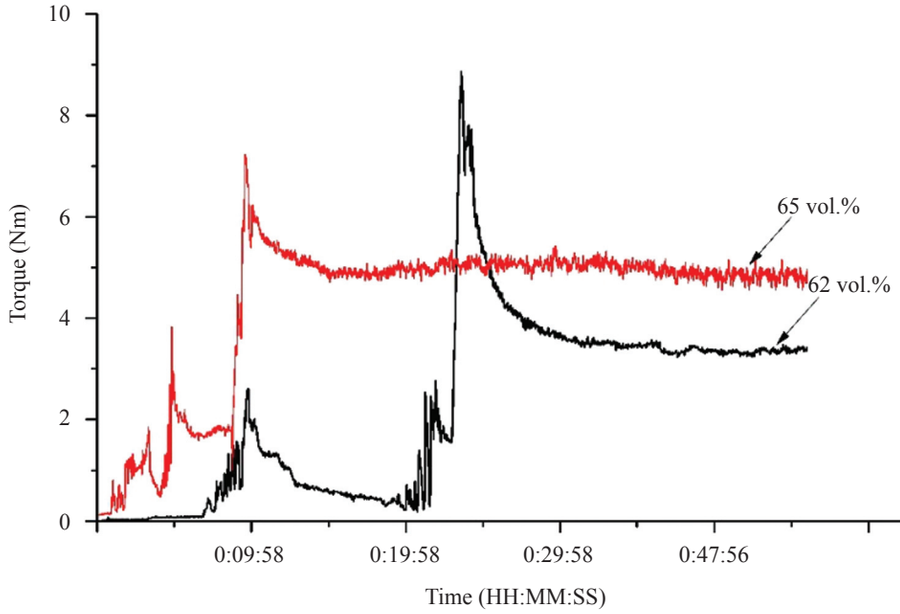

FIGURE 10. The effect of powder loading on the Torque

CHARACTERISTICS OF FEEDSTOCK: RHEOLOGICAL PROPERTIES

Figure 11 illustrates the outcomes pertinent to the feedstock's rheological measurements at three temperature points of 130, 140 and 150°C. Rheology graphs shown in Figure 11 reveal pseudoplastic behaviour at specific thermal points of 130, 140 and 150°C, while the monomodal and bimodal feedstocks speed goes down with shear rate at the afore-mentioned temperatures. Shear thinning, known as pseudoplastic behavior, is useful for μPIM. In other words, the increase of viscosity with shear rate which happens because of dilatant behavior was not observed. Nevertheless, regarding all the samples, the reduction in viscosity level begins when the temperature reaches to 150°C. That is a consequent of a larger binder expansion as well as disentanglement of the molecular chain while the heating process is ongoing that we witness reduction of powder volume (Liu et al. 2001).

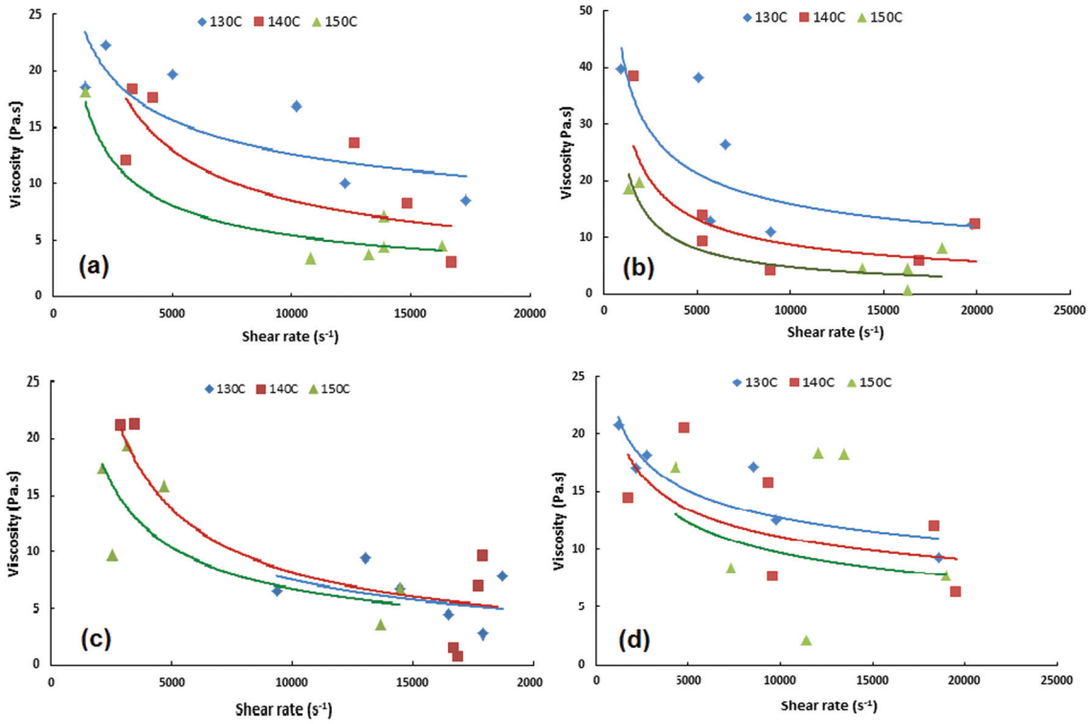

FIGURE 11. Relation between viscosity and shear rate of (a) micro powder (b) 10% nano powder (c) 20% nano powder (d) 30% nano powder in PEG feedstock

As German and Bose (1997) reported, flow that exhibits a viscosity of less than 1000 Pa·s in the shear rate range between 10^2 s^{-1} and 10^5 s^{-1} is needed for PIM. For low-pressure moulding techniques, which is utilized in µPIM process, viscosity must be lower than 45 Pa·s (German & Bose 1997). The viscosity for all of the samples was less than 45 Pa·s, which confirms that the flow behavior of the feedstock satisfies the µPIM process requirements. Lower viscosity value provides easier feedstock flow. The obtained viscosity data shows the flowability of the feedstock. In addition, viscosity links shear stress and shear strain rate. Notably, rheology is included in the description of mechanical properties of various materials under various deformation conditions in which these materials tend to flow. Rheological evaluations of powder–binder mixtures aim to isolate conditions leading to flow instabilities, whether these instabilities are caused by the binder, moulding temperature, powder loading, shear rate, or tool design. Rheological evaluation also serves as a quality control tool in a PIM operation.

The flow behaviour exponent value 'n' indicates the shear sensitivity degree. Generally speaking, the viscosity (η) of non-Newtonian fluids is a function of shear rate (γ) and can be described by Equation 2 (Huang et al. 2003):

$$\eta = k\gamma^{n-1} \quad (3)$$

where n is the flow index and k is a constant. The flow behavior exponent value n indicates the shear sensitivity degree. Any increase in temperature results in the increase in pseudoplasticity of the feedstock. Lower n value means faster change in the viscosity of the feedstock with shear rate. Flow behavior index can be easily calculated by considering the gradient of the obtained graphs. The results for flow behavior index are given in range of 0.25 to 0.76.

Table 4 shows the values of n at each composition and temperature of different powders. Overall, the n values obtained are less than 1, which shows that the feedstock has high pseudoplastic properties, thereby facilitating PIM (Li & Norhamidi 2011). A lower value of n means the more sensitive the viscosity is against shear rate. In turn, higher n the value indicates slower change in viscosity with shear rate.

The change in relative viscosity with composition (% of small particles) for a bimodal mixture at a solid loading of 62% is shown in Figure 11. Based on Figure 11(b), which contains 10% nanopowder, nanopowders initially cause increased viscosity and powder loading, even increased high injection temperature, because of high surface area. However, for samples with 20% and 30% nanopowder, viscosity decreased, which is consistent with the result obtained by German and Bose (German & Bose 1997). Relative viscosity initially decreases, and then reaches a minimum point prior to increasing again with continued addition of smaller particles.

EFFECTS OF NANOPOWDER ON RHEOLOGICAL BEHAVIOR

The change in relative viscosity with the composition (% of small particles) for a bimodal mixture at a solids loading of 62% is shown in Figure 11. Based on reported results in 11(b), which shows the sample containing 10% nanopowder, nanopowders caused increased viscosity and powder loading,

as well as increased high injection temperature, because of high surface area. However, the samples with 20% and 30% nanopowder showed decreased viscosity. Such result agrees with the reports by German and Bose (1997) and Heaney (2012) Relative viscosity initially decreases, thus reaching a minimum point prior to re-increasing with continued addition of smaller particles. In addition, powders with large differences in particle size can be tailored to improve the packing density and decrease the viscosity of the feedstock for any given fixed solid loading.

TABLE 4. Values of n for each feedstock at different temperatures

Sample	Temperature (°C)	n
micro powder	130	0.58
	140	0.41
	150	0.27
10 % nano powder	130	0.70
	140	0.40
	150	0.42
20 % nano powder	130	0.33
	140	0.25
	150	0.38
30 % nano powder	130	0.76
	140	0.72
	150	0.66

The shape of the metal particles also has a significant effect on the relative viscosity of the feedstock (Heaney 2012). Irregularly shaped powders, such as the micropowders used in this study, result in feedstock with high viscosity because of high interparticle friction and low packing density. Small spherical powders are ideal for injection moulding because of their good flowability and low interparticle friction. Therefore, in the present study, a mixture of irregular and spherical powders was selected to be used in a bimodal system (Heaney 2012). Based on the determined packing density, CPVC, and feedstock behavior, a hybrid nano- and micropowder mixture can be utilized to produce a cost-effective feedstock with low viscosity. According to the rheological analysis, the powder and binder mixture exhibits pseudoplastic behavior. Thus, the obtained feedstock based on PEG meets the primary requirements of flow characteristics. With regard to viscosity, this feedstock generally shows values below 45 Pa·s, which means that this feedstock can satisfy the μPIM criteria.

EFFECTS OF NANOPOWDER ON RHEOLOGICAL BEHAVIOR

Temperature is one of the important factors in injection moulding. Selection of inappropriate temperature during injection moulding produces disability to the sintered part. Therefore, rheological experiments provide fluid properties at a given temperature based on the viscosity of the fluid. The increase in temperature reduces the viscosity of the feedstock, because binder bonding decomposes at high temperatures.

Equation 4 relates temperature and viscosity, wherein the value of the activation energy E is used. E refers to the sensitivity of the feedstock to temperature changes during the injection process. E must be sufficiently low to facilitate feedstock flow into the mould before hardening.

$$\eta = \eta_0 \exp(E/RT) \quad (4)$$

Figure 12 shows the viscosity at shear rates of 5000, 10000 and 15000 s^{-1}. Gradients can be used to obtain the value of E for the viscosity gradient, η (Pa·s) versus temperature, 1/T (K^{-1}) is equal to E/R, where R is the gas constant, 8.314472 J/K·mol. Thus, the activation energy values obtained are shown in Table 5.

TABLE 5. Values of activation energy E for monomodal and bimodal feedstock with PEG based binder system

Sample	Shear rate (s^{-1})	Activation Energy (J/K.mol)
micro powder	5000	66.52
	10000	81.76
	15000	85.22
10 % nano powder	5000	45.73
	10000	57.50
	15000	65.13
20 % nano powder	5000	6.24
	10000	7.62
	15000	12.47
30 % nano powder	5000	13.85
	10000	18.71
	15000	20.79

E was increased when the shear rate value was increased up to 15000 s^{-1}. As presented in Table 4, the obtained E values are lower for bimodal samples than the monomodal sample, whereas E decreased from 85.22 J/K·mol to 6.24 J/K·mol. A low value of E is required to prevent the occurrence of any defects such as distortion and cracking during the final part (Li & Norhamidi 2011). Although the flow activation energy is just a little, it is desirable for good filling behaviour in order to prevent sharp viscosity fluctuations and mitigating the flow ability of the feedstock leading to stress concentration, distortion and cracking in the mould specimens. Furthermore, a weak temperature-dependence viscosity is helpful to avoid shrinkage-related defects by allowing more pressure transmission to the cavity (Huang et al. 2003). Defect-free injected parts are shown in Figure 13, in which the injected (green) part was produced without any physical defects, such as short shot, cracks and sink mark. A defect-free microsample with 30 wt.% nanopowder was obtained by low-temperature injection at 85°C under approximately 0.8 MPa pressure. The injection temperature for feedstock that contains the micropowder was 130°C with 0.8 MPa pressure, which means that injection temperature was decreased by around 40% compared with that for the microparts fabricated using micropowder feedstock. The result is also comparable with that obtained with the use of SS 316L powder in the μPIM process. Results at this stage confirm that a PEG binder system, along with nano–micro-sized powder, can be used as a binder to produce low-viscosity and low-temperature feedstock in μPIM.

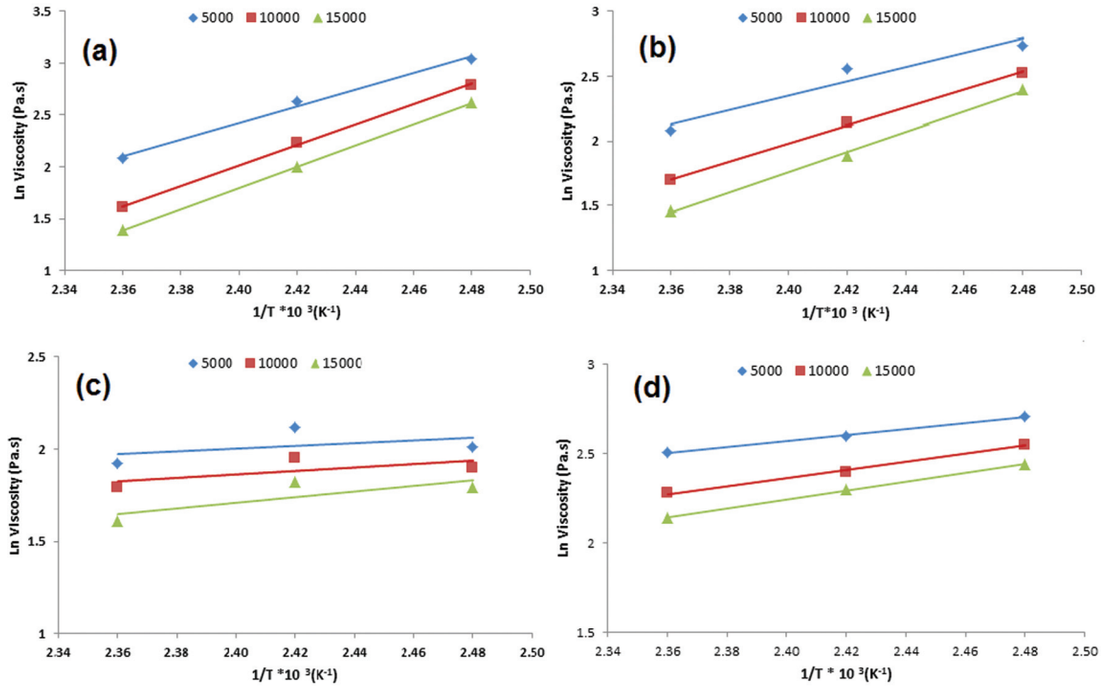

FIGURE 12. Relationship viscosity against temperature for feedstocks (a) micro powder (b) 10% nano powder (c) 20% nano powder (d) 30% nano powder in PEG feedstock

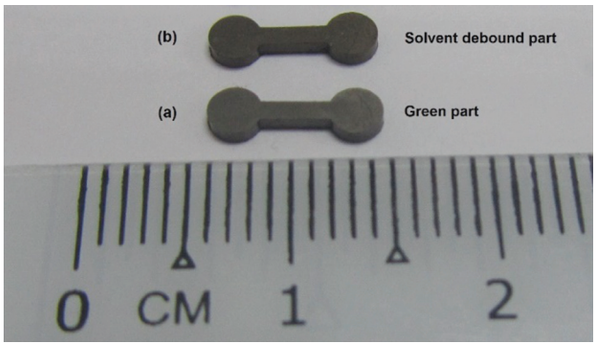

FIGURE 13. Defect-free microinjection moulded part (tensile bar specimen)

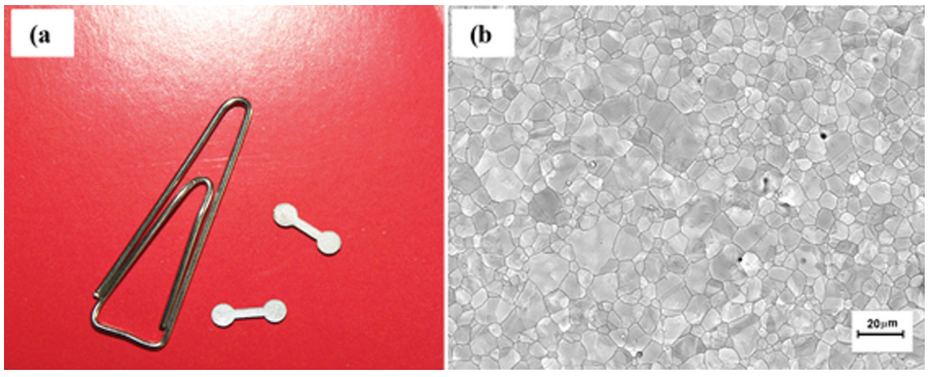

FIGURE 14. Images of (a) sintered sample and (b) surface microstructure

According to German and Bose (1997), the minimum strength of the injected part must be 5 MPa. The flexure stress for microparts consisting of micropowder with 15.54 MPa increased to 21.83 MPa for samples consisting of 30 wt.% nanopowder. The next significant aspect for green parts is density. Nanopowder addition increases density from 5.178 g/cm^3 to 5.328 g/cm^3 because bimodal system powder shows increased powder loading, resulting in an increase in packing density of injected parts. Density must be near 5 g/cm^3 for a feedstock. Therefore, green density and strength of microinjected parts using nano-micro hybrid powder mixtures can be increased in comparison with that for micropowders, because bimodal system powders can increase powder loading, resulting in increased packing density of the injected parts. These results showed that the obtained results for injected parts in this work are the approximate mechanical properties of an ideal green part.

As shown in Figure 14, uniform structure, low porosity, and a grain size of less than 10 μm is achieved for samples containing nanopowder (30%) sintered at 1200°C for 1 h. Activated sintering of stainless steel nanopowders occurred at lower temperatures below micropowders due to high surface area energy. By using nanopowders with refined grain microstructure, hardness increased from 182 HV to 221 HV. In addition, adding nanosized to micropowders induced an increase in microcomponent strength from 435 MPa to 501 MPa, having 97% theoretical density.

CONCLUSION

The addition of nanopowder into micropowder increased the CPVC of the feedstock. The results of the rheology analysis show that the binder–powder mixture exhibits pseudoplastic behavior. The obtained feedstock generally shows viscosity values below 45 Pa·s, which means that this feedstock satisfies the requirements for μPIM. The flow behavior index of the feedstock ranges between 0.25 and 0.76. For samples that contain 10% nanopowder, their viscosity and powder loading increases initially because of high surface area. However, for samples with 20% and 30% nanopowder, their viscosity was decreased. The obtained E values for bimodal samples were lower than that of monomodal samples; E decreased from 85.22 J/K·mol to 6.24 J/K·mol. A defect-free microsample with 30 wt.% nanopowder was obtained by low-temperature injection at 85°C, with flexure stress of 15.54 MPa and green part density of 5.178 g/cm^3. In addition, the sintered parts showed uniform structure, low porosity, and grain size of less than 10 μm, along with hardness of 221 HV, strength of 501 MPa, and exhibiting 97% theoretical density. Based on the determined CPVC and feedstock behavior, as well as the mechanical properties of injected and sintered parts, hybrid nano- and micropowders can be utilized to produce a feedstock with low viscosity at low temperature for μPIM.

ACKNOWLEDGEMENT

This work was conducted under Projects number P.Sh/10/3729 of Islamic Azad University, Gonbad Kavoos branch.

REFERENCES

Abolhasani, H. & Muhamad, N. 2010. A new starch-based binder for metal injection molding. *Journal of Materials Processing Technology* 210(6-7): 961-968.

Attia, U.M. & Alcock, J.R. 2011. a review of micro-powder injection moulding as a microfabrication technique. *Journal of Micromechanics and Microengineering* 21(4): 43001-43022.

Emeka, U.B., Sulong, A.B., Muhamad, N., Sajuri, Z. & Salleh, F. 2017. Two component injection moulding of bi-material of stainless steel and yttria stabilized zirconia–green part. *Jurnal Kejuruteraan* 29(1): 49-55.

German, R.M. & Bose, A. 1997. *Injection Molding of Metals and Ceramics*. Princeton, New Jersey: Metal Powder Industries Federation.

Hashim, J., Looney, L. & Hashmi, M. 2002. Particle distribution in cast metal matrix composites–Part I. *Journal of Materials Processing Technology* 123(2): 251-257.

Heaney, D.F. 2012. *Handbook of Metal Injection Moulding*. Cambridge, UK: Woodhead Publishing.

Huang, B., Fan, J., Liang, S. & Qu, X. 2003. The Rheological and sintering behavior of nano-structured crystalline powder. *Journal of Materials Processing Technology* 137(1-3): 177-182.

Huang, C.-L., Wang, J.-J. & Huang, C.-Y. 2005. Sintering behavior and microwave dielectric properties of nano alpha-alumina. *Materials Letters* 59(28): 3746-3749.

Ibrahim, M.H.I., Muhamad, N. & Sulong, A.B. 2009. Rheological investigation of water atomised stainless steel powder for micro metal injection molding. *International Journal of Mechanical and Materials Engineering* 4(1): 1-8.

Ibrahim, M.H.I., Muhamad, N., Sulong, A.B., Jamaludin, K.R., Ahmada, S. & Norb, N.H.M. 2010. Optimization of micro metal injection molding for highest green strength by using taguchi method. *International Journal of Mechanical and Materials Engineering* 5(2): 282-289.

Ismail, M.H., Muhamad, N. & Omar, M.A. 2008. Characterization of Metal Injection Molding (MIM) feedstock based on water soluble binder system. *Jurnal Kejuruteraan* 20: 11-18.

Jamaludin, K.R., Muhamad, N., Rahman, M.N.A., Murtadhahadi, Ahmad, S., Ibrahim, M.H.I. & Nor, N.H.M. 2009. Rheological investigation of water atomized metal injection molding (MIM) feedstock for processability prediction. *Advanced Materials Research* 83-86: 945-952.

Javad, R., Norhamidi, M. & Sulong, A.B. 2012. Effect of nano-sized powders on powder injection molding: A review. *Microsystem Technologies* 18(12): 1941-1961.

Javad, R., Norhamidi, M., Sulong, A.B., Hasyimah, A., Fayyaz, A. & Zakaria, H. 2013. Characterization of fabricated feedstock using nano powders and a water-soluble binder in micro metal injection molding. *Journal of Nano Research* 25: 174-180.

Li, H.P. & Norhamidi, M. 2011. Rheological analysis of microminiature powder injection molding (MPIM) feedstock. *Applied Mechanics and Materials* 52-54: 238-243.

Liu, Z.Y., Loh, N.H., Tor, S.B., Khor, K.A., Murakoshi, Y. & Maeda, R. 2001. Binder system for micropowder injection molding. *Materials Letters* 48(1): 31-38.

Martin, C. & Bouvard, D. 2004. Isostatic compaction of bimodal powder mixtures and composites. *International Journal of Mechanical Sciences* 46(6): 907-927.

Merz, L., Rath, S., Piotter, V., Ruprecht, R., Ritzhaupt-Kleissl, J. & Hausselt, J. 2002. Feedstock development for micro powder injection molding. *Microsystem Technologies* 8(2-3): 129-132.

Onbattuvelli, V.P., Enneti, R.K., Park, S.-J. & Atre, S.V. 2013. The effects of nanoparticle addition on sic and aln powder–polymer mixtures: packing and flow behavior. *International Journal of Refractory Metals and Hard Materials* (36): 183-190.

Quinard, C., Barriere, T. & Gelin, J.C. 2009. Development and property identification of 316l stainless steel feedstock for PIM and μPIM. *Powder Technology* 190(1-2): 123-128.

Shi, J.L. & Zhang, J. 2000. Compaction and sintering behavior of bimodal alumina powder suspensions by pressure filtration. *Journal of the American Ceramic Society* 83(4): 737-742.

Suri, P., Atre, S.V., German, R.M. & de Souza, J. P. 2003. Effect of mixing on the rheology and particle characteristics of tungsten-based powder injection molding feedstock. *Materials Science and Engineering: A* 356(1-2): 337-344.

Trunec, M. & Maca, K. 2007. Compaction and pressureless sintering of zirconia nanoparticles. *Journal of the American Ceramic Society* 90(9): 2735-2740.

Trunec, M., Maca, K. & Shen, Z. 2008. Warm pressing of zirconia nanoparticles by the spark plasma sintering technique. *Scripta Materialia* 59(1): 23-26.

Wetzel, K., Rixecker, G., Kaiser, G. & Aldinger, F. 2005. Preparation of dense nanocrystalline silicon carbide ceramics by sinter forging in the presence of a liquid phase. *Advanced Engineering Materials* 7(6): 520-524.